

# 3<sup>rd</sup> International Conference on Chemo and BioInformatics Kragujevac, September 25-26, 2025, Serbia



## ICCBIKG 2025

International Conference  
on Chemo and BioInformatics

## Book of Proceedings

### ORGANIZERS AND SPONSORS



Republic of Serbia

MINISTRY OF SCIENCE,  
TECHNOLOGICAL DEVELOPMENT AND INNOVATION

**MC LABOR**  
LABORATORIJSKA I PROCESNA OPREMA



Hitachi High-Tech

**SUPERLAB**  
Your lab - Our passion



**KPM**  
ANALYTICS  
Authorized Distributor

**EQUILAB**

**ANALYSIS**  
LABORATORY EQUIPMENT

3<sup>rd</sup> International Conference on Chemo and BioInformatics  
ICCBIKG 2025

# BOOK OF PROCEEDINGS

September 25-26, 2025  
Kragujevac, Serbia

Sponsored by



Anton Paar

Hitachi High-Tech



EQUILAB



**SUPERLAB**<sup>®</sup>  
Your lab - Our passion



3<sup>rd</sup> International Conference on Chemo and BioInformatics, Kragujevac, September 25-26, 2025, Serbia.

**Editors:**

Dr. Igor Saveljić

Prof. Dr. Nenad Filipović

**Technical Editors:**

Dr. Vladimir Simić

Dr. Marko Antonijević

**Proofreading:**

Kristina Milisavljević

**Press:**

„Grafo Ink“, Kragujevac

**Impression:**

10 copies

**Publisher:**

Institute for Information Technologies, University of Kragujevac, Serbia, Jovana Cvijića bb, 2025

CIP - Каталогизacija у публикацији Народна библиотека Србије, Београд

54:004(048)(0.034.2)  
57+61]:004(082)(0.034.2)

INTERNATIONAL Conference on Chemo and BioInformatics (3 ; 2025 ; Kragujevac)  
Book of Proceedings [Elektronski izvor] / 3rd International Conference on Chemo and  
BioInformatics, ICCBIKG 2025, September 25-26, 2025, Kragujevac, Serbia ; [editors Igor Saveljić,  
Nenad Filipović]. - Kragujevac : University, Institute for Information Technologies, 2025  
(Kragujevac : Grafo Ink). - 1 USB fleš memorija ; 1 x 2 x 3 cm

Sistemska zahtevi: Nisu navedeni. - Nasl. sa naslovne strane dokumenta. - Tiraž 10. - Bibliografija  
uz svaki rad.

ISBN 978-86-82172-05-5

a) Хемија -- Информациона технологија -- Зборници b) Биомедицина -- Информациона  
технологија -- Зборници

COBISS.SR-ID 176312073

# Organized by:

Institute for Information Technologies, University of Kragujevac, **Organizer**



The Ministry of Science, Technological Development and Innovation of The Republic of Serbia, *Supporting organization*



University of Kragujevac, *Suborganizer*



Faculty of Medicinal Sciences, University of Kragujevac, *Suborganizer*



Faculty of Science, University of Kragujevac, *Suborganizer*



Institute for Biological Research "Siniša Stanković" - National Institute of Republic of Serbia, University of Belgrade, *Supporting organization*



Serbian Chemical Society, *Supporting organization*



## ***In Silico* investigation of substitution mechanism at the Nickel carbonyl complex**

Dušan S. Čoćić<sup>1\*</sup>, Biljana V. Petrović<sup>1</sup>, Ana S. Kesić<sup>2</sup>

<sup>1</sup> Faculty of Science, University of Kragujevac, Kragujevac, Serbia;

e-mail: [dusan.cocic@pmf.kg.ac.rs](mailto:dusan.cocic@pmf.kg.ac.rs)

<sup>2</sup> Institute for Information Technologies, University of Kragujevac, Kragujevac, Serbia;

e-mail: [akesic@uni.kg.ac.rs](mailto:akesic@uni.kg.ac.rs)

\*Corresponding author: [dusan.cocic@pmf.kg.ac.rs](mailto:dusan.cocic@pmf.kg.ac.rs)

DOI: 10.46793/ICCBiKG25.660C

**Abstract:** The reaction mechanism of carbon monoxide substitution at the tetracarbonyl nickel complex was studied in depth by DFT calculations. Substituents used in these reactions were hydrogen cyanide, pyridine, trimethylamine, trimethylphosphine, triphenylphosphane, and trimethylarsine, as well as carbon monoxide for the carbon monoxide exchange reaction. To investigate the reaction mechanism, reaction energy, reaction force, and reaction force constant profile were calculated. Additionally, changes of electron density at bond critical points of a breaking and a forming bond were monitored along the reaction. All gathered data were further statistically analyzed in order to find a possible correlation between them. Results gained in this way point out details that could not be observed by conventional experimental investigations of reaction kinetics and mechanisms but certainly should be taken into account in further designing of suitable complexes for desirable reactions.

**Keywords:** Nickel tetracarbonyl complex, reaction force analysis, reaction electronic flux (REF), AIM topology analysis, Data analysis.

### **1. Introduction**

Nickel tetracarbonyl [Ni(CO)<sub>4</sub>], also known as nickel carbonyl, is a key compound in the industrial process of refining nickel and producing nickel-based catalysts. It is used in the Mond process, which involves nickel ore reacting with carbon monoxide to form nickel tetracarbonyl, which is then decomposed to produce high-purity nickel. Additionally, nickel tetracarbonyl serves as a catalyst precursor for various chemical reactions, including the production of polyethylene and other plastic. Therefore, understanding the chemical reactions in which nickel tetracarbonyl plays a significant role (as a reactant or catalyst) can be regarded as a cornerstone for further development and improvement of akin reactions. Thus, in this report we have performed a thorough *in silico* investigation of carbon monoxide substitution at the nickel tetracarbonyl complex by CO, HCN, Pyridine (Py), trimethylamine (NMe<sub>3</sub>), trimethylphosphine (PMe<sub>3</sub>), triphenylphosphane (PPh<sub>3</sub>) and trimethylarsine (AsMe<sub>3</sub>) ligands. These reactions were studied in detail by applying conceptual density functional theory. This approach enabled us to gain further insight into the underlying reaction mechanism at the microscopic level (involving only direct participants of the reaction, without the

influence of solvent) and to put the concept of the reaction mechanism on a quantitative basis.

## 2. Methodology

Optimization of all complex structures (reactants, products, and transition states) for comprising reasons was performed at b3lyptheory level in combination with the 6-311+g(d,p) basis set. All structures were characterized as local minima or true transition states by computation of vibration frequencies at the same theory level combinations. The minimum energy path going from the reactant to the product was calculated at the b3lyp/6-311+g(d,p) through the intrinsic reaction coordinate (IRC). The GAUSSIAN suite of programs was used. Topology analysis was performed using AIMAll software.

## 3. Results and Discussion

The reactions of carbon monoxide substitution at the tetracarbonyl nickel complex by selected ligands were studied throughout the reaction path presented in Figure 1.

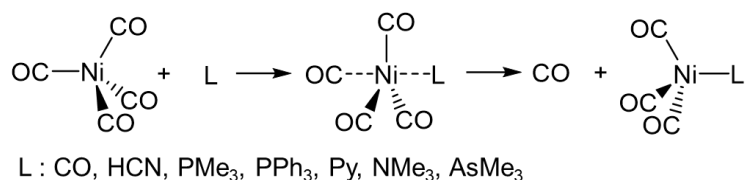


**Figure 1.** Reaction path of CO ligand substitution reactions at Ni<sup>0</sup> tetracarbonyl complex.

Calculated reaction energy profiles have provided us with reaction activation energies ( $\Delta E^\ddagger$ ) and the reaction energies ( $\Delta E^\circ$ ). From reaction energy profiles, the reaction force profiles and reaction force constant profiles have been calculated. Reaction force profiles provide natural partitions of the reaction diagrams into three chemical regions, which gives the possibility to put the concept of reaction mechanisms on a quantitative basis. Each of these regions is predominantly (but not exclusively) governed by different chemical events, wherein in the transition state regions most of the electronic events (such as bond breaking/forming and charge redistribution) are accentuated, while the geometrical events (changes in bond lengthening, rotations, etc.) are mainly emphasized during the reactant and product regions. The amount of energy involved in all those stages might be quantified through the amount of work done on the system within different regions. Reaction works  $W_1$  and  $W_4$  are defined in the reactant and product regions, they are mostly accounting for structural rearrangements, whereas  $W_2$  and  $W_3$  defined within the transition state region, are mostly due to electronic effects. Calculated values of described reaction work energies together with reaction activation energies and the reaction energies are summarized in Table 1. Additionally, changes of electron density at bond critical points of a breaking (bond Ni-C) and a forming (bond Ni-L) bond were monitored along the reaction. It was observed that those changes follow an

exponential decay or growth pattern, so they were accordingly fitted, and the exponential parameters were presented in Table 1.

**Table 1.** Calculated energetic properties associated with the reactions under study together with exponential fitting parameters of electron density change at BCPs for presented bonds.

Ligand	Energy (kcal/mol)						bond Ni-C		bond Ni-L	
	$\Delta E^\ddagger$	$\Delta E^\circ$	$W_1$	$W_2$	$W_3$	$W_4$	$a^a$	$b^b$	$a^a$	$b^c$
CO	19.37	0.00	6.64	12.73	-11.20	-8.17	0.46	7.71	0.00	7.71
HCN	19.34	12.47	6.74	12.60	-4.20	-2.67	0.53	7.40	0.00	6.51
Py	17.99	9.34	9.56	8.43	-4.61	-4.04	1.12	8.98	0.00	4.75
NMe <sub>3</sub>	18.00	10.93	9.19	8.81	-3.60	-3.47	0.94	7.30	0.00	3.83
PMe <sub>3</sub>	16.82	0.94	10.21	6.61	-9.80	-6.08	1.96	7.75	0.00	4.26
PPh <sub>3</sub>	17.38	1.97	9.40	7.98	-9.27	-6.14	3.69	9.63	0.00	4.78
AsMe <sub>3</sub>	17.24	3.52	10.62	6.62	-7.73	-5.99	2.29	8.08	0.00	3.96

<sup>a</sup>Initial value of a exponential fi

<sup>b</sup>Exponential decay rate

<sup>c</sup>Exponential growth rate

In order to find possible correlations between the calculated data presented in Table 1 and to better understand the investigated reaction series, further data analysis was performed. Thus, the Pearson product-moment correlation coefficient ( $r$ ) was used to measure the strength of the linear relationship between variables presented in Table 1. Calculated values of  $r$  correlation coefficients between selected data presented in Table 1 are summarized in Table 2.

**Table 2.** Pearson correlation coefficients matrix (green field ( $|r| \geq 0.85$ ) - strong linear relationship, yellow field ( $0.80 \geq |r| \geq 0.85$ ) - medium linear relationship)

	$\Delta E^\ddagger$	$\Delta E^\circ$	$W_1$	$W_2$	$W_3$	$W_4$	$a$	$b$	$a$	$b$
$\Delta E^\ddagger$	1.00	0.35	-0.96	0.98	0.18	0.13	-0.75	-0.38	-0.80	0.86
$\Delta E^\circ$	0.35	1.00	-0.20	0.26	0.98	0.96	-0.47	-0.28	0.09	-0.12
$W_1$	-0.96	-0.20	1.00	-0.99	0.00	-0.03	0.64	0.36	0.90	-0.92
$W_2$	0.98	0.26	-0.99	1.00	0.07	0.07	-0.69	-0.37	-0.87	0.91
$W_3$	0.18	0.98	0.00	0.07	1.00	0.95	-0.37	-0.21	0.29	-0.31
$W_4$	0.13	0.96	-0.03	0.07	0.95	1.00	-0.29	-0.21	0.21	-0.29
$a$	-0.75	-0.47	0.64	-0.69	-0.37	-0.29	1.00	0.72	0.36	-0.52
$b$	-0.38	-0.28	0.36	-0.37	-0.21	-0.21	0.72	1.00	0.22	-0.19
$a$	-0.80	0.09	0.90	-0.87	0.29	0.21	0.36	0.22	1.00	-0.93
$b$	0.86	-0.12	-0.92	0.91	-0.31	-0.29	-0.52	-0.19	-0.93	1.00

The Pearson correlation coefficients matrix (Table 2) tells us that the activation energy barrier  $\Delta E^\ddagger$  is mostly influenced by reaction works  $W_1$  and  $W_2$  and by the electron density growth rate of a forming bond. Thus, in order to manipulate the activation energy barrier, for example, to lower one of their values, one must choose an entering ligand that, in the reaction of carbon monoxide substitution at  $\text{Ni}(\text{CO})_4$ , exhibits a greater

amount of reaction work needed for structural rearrangement ( $W_1$ ) and/or needs a lower amount of  $W_2$  and/or has a slower growth rate of electron density of a forming bond. Values of reaction energies ( $\Delta E^\ddagger$ ) for this substitution series are predominantly influenced by reaction works  $W_3$  and  $W_4$ . Those reaction works have a positive correlation to reaction energies, meaning that with increasing of its values, reaction energy also increases. An interesting correlation was also found between reaction works  $W_1$  and  $W_2$  and the growth rate of electron density of a forming bond. Reaction work  $W_1$  has a negative correlation, while reaction work  $W_2$  has a positive correlation with the electron density growth rate of the forming bond. Thus, meaning that the faster electron density growth needs more energy for the electron rearrangement process ( $W_2$ ), while, on the contrary, there is less work needed for the structural rearrangement process ( $W_1$ ).

#### 4. Conclusions

Even though donor atoms of the entering ligand differ in their chemical nature, they yield only minor differences in the activation energy barrier. The standard deviation between  $\Delta E^\ddagger$  of the investigated reaction was calculated to be only 0.93 kcal/mol. Therefore, additional analyses of reaction mechanisms were performed. Throughout this analysis it was found that all investigated reactions go through a multi-stage, one-step reaction mechanism by which the substitution starts with a bond formation/strengthening process followed by a bond breaking/weakening process. Reaction energy barriers have a negative correlation with reaction work needed for structural rearrangement of reactants and a positive correlation with reaction work needed for electronic rearrangement prior to reaching a transition state point. In general, reactions in which substituent ligands are the ones with nitrogen as a donor atom (HCN, Py, and NMe<sub>3</sub>) have been characterized as the most endergonic. Total reaction energies for this substitution series have a positive correlation with the reaction work released during structural and electronic relaxation processes.

#### Acknowledgment

This research is funded by the Ministry of Education and Ministry of Science, Technological Development and Innovation, Republic of Serbia, Grants: No. 451-03-136/2025-03/200378 and 451-03-136/2025-03.

#### References

- [1] A. D. Becke, *J. Phys. Chem.*, (1993) 98, 5648-5652.
- [2] W.J. Hehre, L. Random, P. v. R. Schleyer, J. A. Pople, Wiley: New York, 1986
- [3] K. Fukui, *Acc. Chem. Res.*, (1981) 14, 363-368.
- [4] Gaussian 09, Revision C.01, M. J. Frisch, et al Gaussian, Inc., Wallingford CT, 2010
- [5] T. A. Keith, AIMAll (Version 13.11.04), TK Gristmill Software, 2013.
- [6] D. Ćoćić, B. Petrović, R. Puchta, M. Chrzanowska, A. Katafias, R. van Eldik, *J. Comput. Chem.*, (2022) 43, 1–15.
- [7] M. R. Buchner, D. Ćoćić, S.I. Ivlev, N. Spang, M. Müllera, R. Puchta, (2023) 52, 5287-5296

**In Silico investigation of substitution mechanism at the Nickel carbonyl  
complex**Dušan S. Ćočić<sup>1\*</sup>, Biljana Petrović<sup>1</sup>, Ana S. Kesić<sup>2</sup>

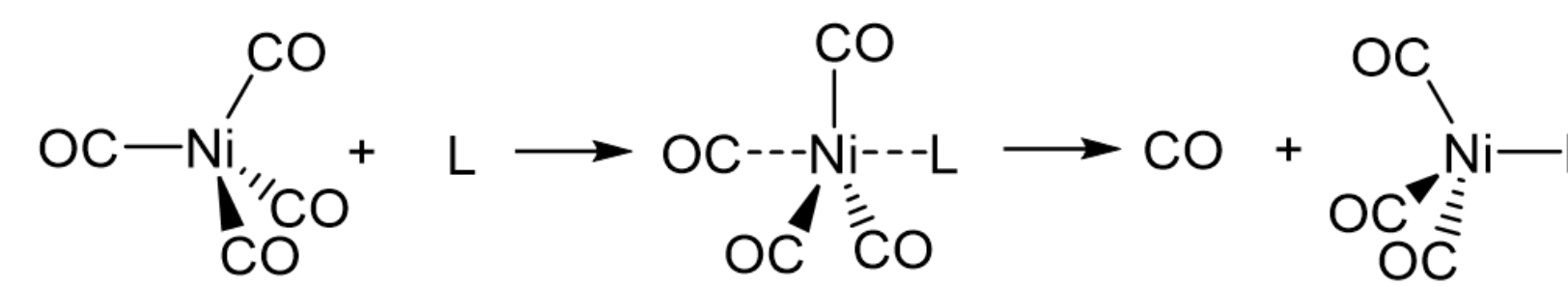
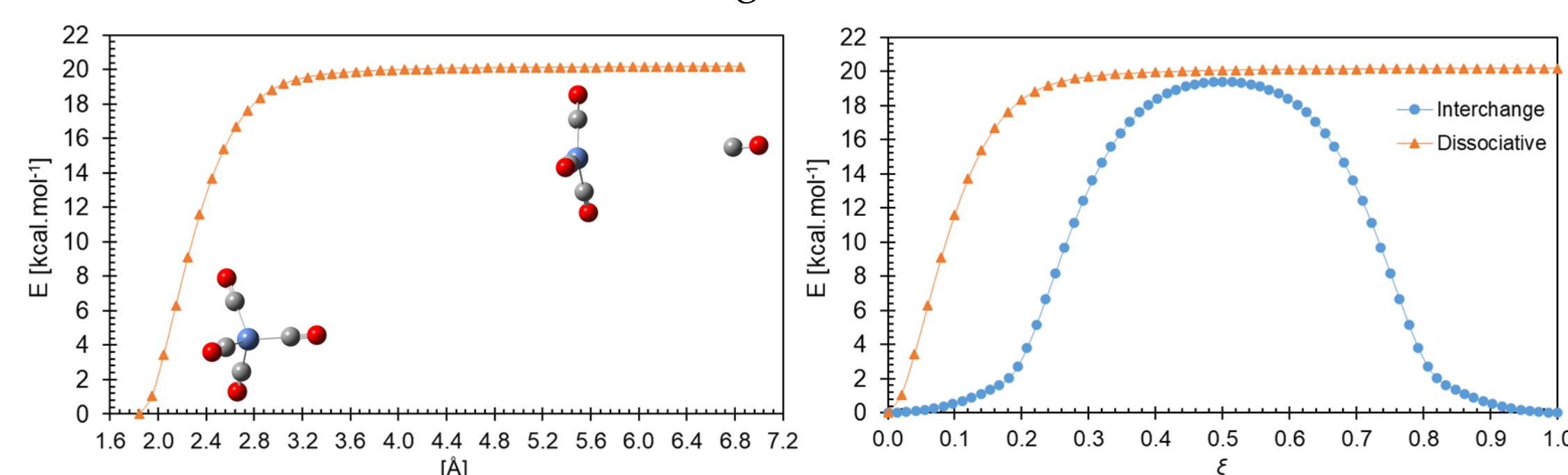
(1) Faculty of Science, University of Kragujevac, Kragujevac, Serbia

(2) Institute for Information Technologies, University of Kragujevac, Kragujevac, Serbia

\*corresponding author e-mail: dusan.cocic@pmf.kg.ac.rs

**Synopsis**

Nickel carbonyl is a key compound in the industrial process of refining nickel and producing nickel-based catalysts. It is used in the Mond process, which involves nickel ore reacting with carbon monoxide to form nickel tetracarbonyl, which is then decomposed to produce high-purity nickel. Additionally, nickel tetracarbonyl serves as a catalyst precursor for various chemical reactions, including the production of polyethylene and other plastics. Therefore, understanding the chemical reactions in which nickel tetracarbonyl plays a significant role (as a reactant or catalyst) can be regarded as a cornerstone for further development and improvement of akin reactions. Thus, in this report we have performed a thorough *in silico* investigation of carbon monoxide substitution at the nickel tetracarbonyl complex by CO, HCN, Pyridine (Py), trimethylamine (NMe<sub>3</sub>), trimethylphosphine (PMe<sub>3</sub>), triphenylphosphane (PPh<sub>3</sub>) and trimethylarsine (AsMe<sub>3</sub>) ligands. These reactions were studied in detail by applying conceptual density functional theory. This approach enabled us to gain further insight into the underlying reaction mechanism at the microscopic level (involving only direct participants of the reaction, without the influence of solvent) and to put the concept of the reaction mechanism on a quantitative basis.

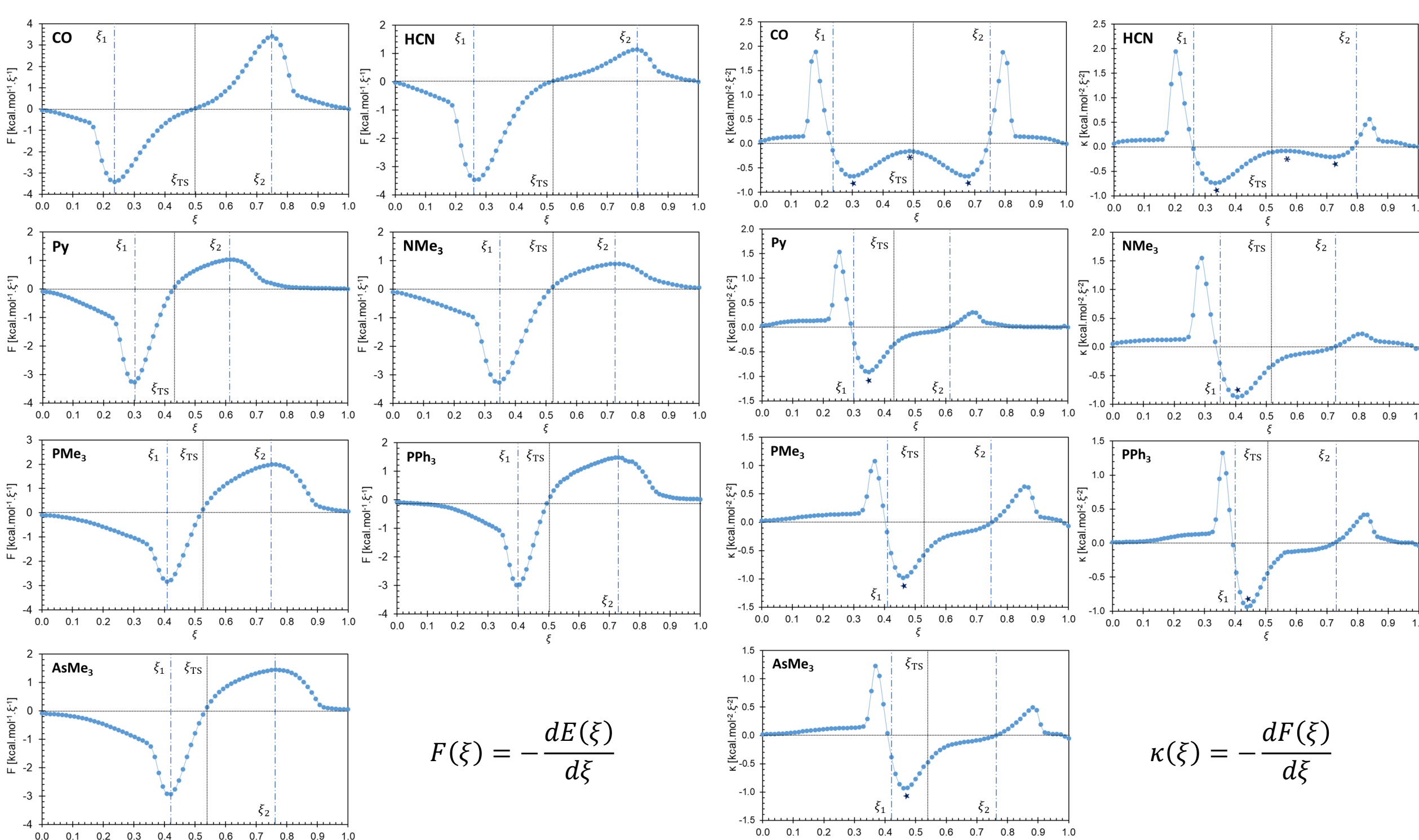
L : CO, HCN, PMe<sub>3</sub>, PPh<sub>3</sub>, Py, NMe<sub>3</sub>, AsMe<sub>3</sub>**Interchange vs Dissociative****Theory**

$$\Delta E^\ddagger = W_1 + W_2 \quad \Delta E^\circ = W_1 + W_2 + W_3 + W_4 \quad J = (J_s - J_{ns}) \quad J(\xi) = -\left(\frac{d\mu(\xi)}{d\xi}\right)$$

$$W_1 = -\int_{\xi_R}^{\xi_1} F(\xi) d\xi > 0; \quad W_2 = -\int_{\xi_1}^{\xi_{TS}} F(\xi) d\xi > 0 \quad J_s = \sum_m \int_{\xi_i}^{\xi_j} |J_m(\xi)| d\xi \text{ for all } J_m(\xi) > 0$$

$$W_3 = -\int_{\xi_{TS}}^{\xi_2} F(\xi) d\xi < 0; \quad W_4 = -\int_{\xi_2}^{\xi_P} F(\xi) d\xi < 0 \quad J_{ns} = \sum_m \int_{\xi_i}^{\xi_j} |J_m(\xi)| d\xi \text{ for all } J_m(\xi) < 0$$

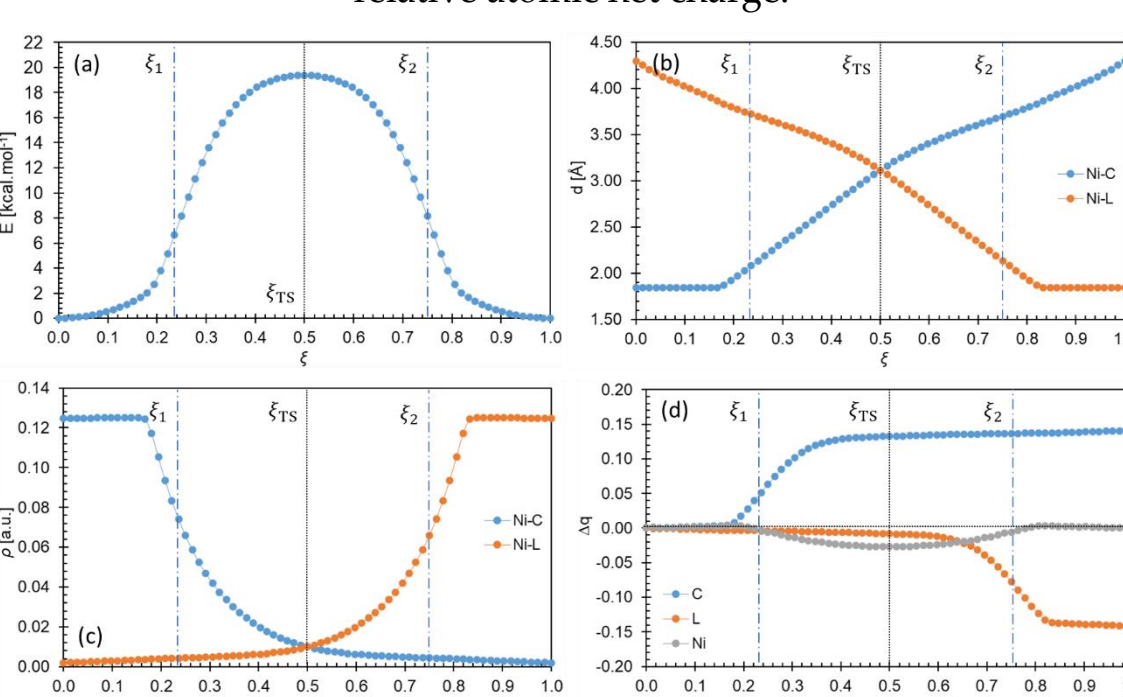
	Energy [kcal/mol]							REF		
	$\Delta E^\ddagger$	$\Delta E^\circ$	$W_1$	$W_2$	$W_3$	$W_4$	%	$J_s$	$J_{ns}$	$J$
CO	19.37	0.00	6.64	12.73	-11.20	-8.17	34.28	25.15	25.15	0.00
HCN	19.34	12.47	6.74	12.60	-4.20	-2.67	34.85	21.50	31.55	-9.93
Py	17.99	9.34	9.56	8.43	-4.61	-4.04	53.14	20.84	24.06	-2.47
NMe <sub>3</sub>	18.00	10.93	9.19	8.81	-3.60	-3.47	51.05	32.40	21.69	10.56
PMe <sub>3</sub>	16.82	0.94	10.21	6.61	-9.80	-6.08	60.70	20.50	27.41	-6.85
PPh <sub>3</sub>	17.38	1.97	9.40	7.98	-9.27	-6.14	54.08	23.86	21.73	2.31
AsMe <sub>3</sub>	17.24	3.52	10.62	6.62	-7.73	-5.99	61.60	19.66	24.59	-4.91



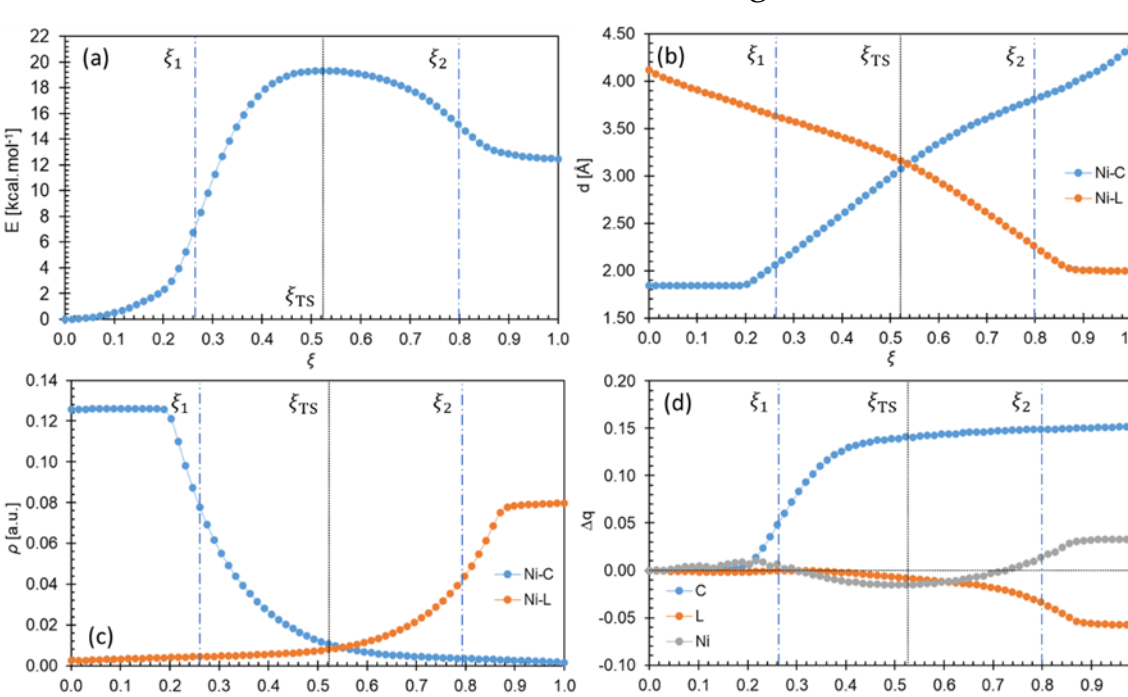
$$F(\xi) = -\frac{dE(\xi)}{d\xi}$$

$$\kappa(\xi) = -\frac{dF(\xi)}{d\xi}$$

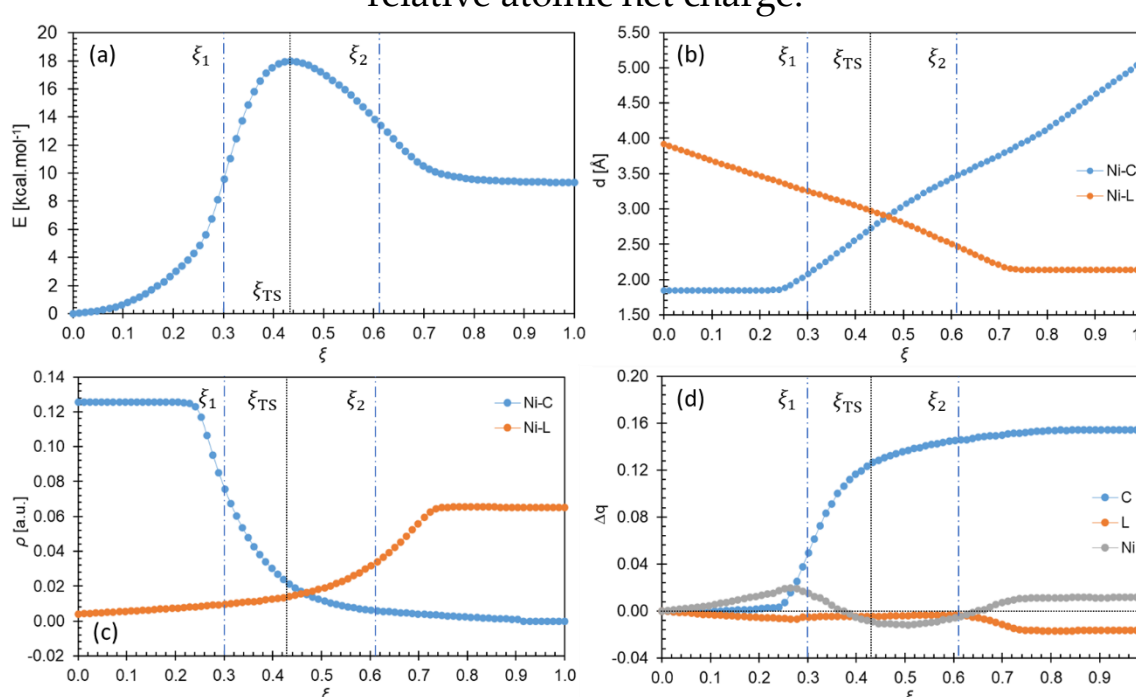
Calculated changes along the reaction path for a carbon monoxide substitution by CO molecule of (a) reaction energy profile, (b) bond distances change, (c) electron density change at BCP and (d) relative atomic net charge.



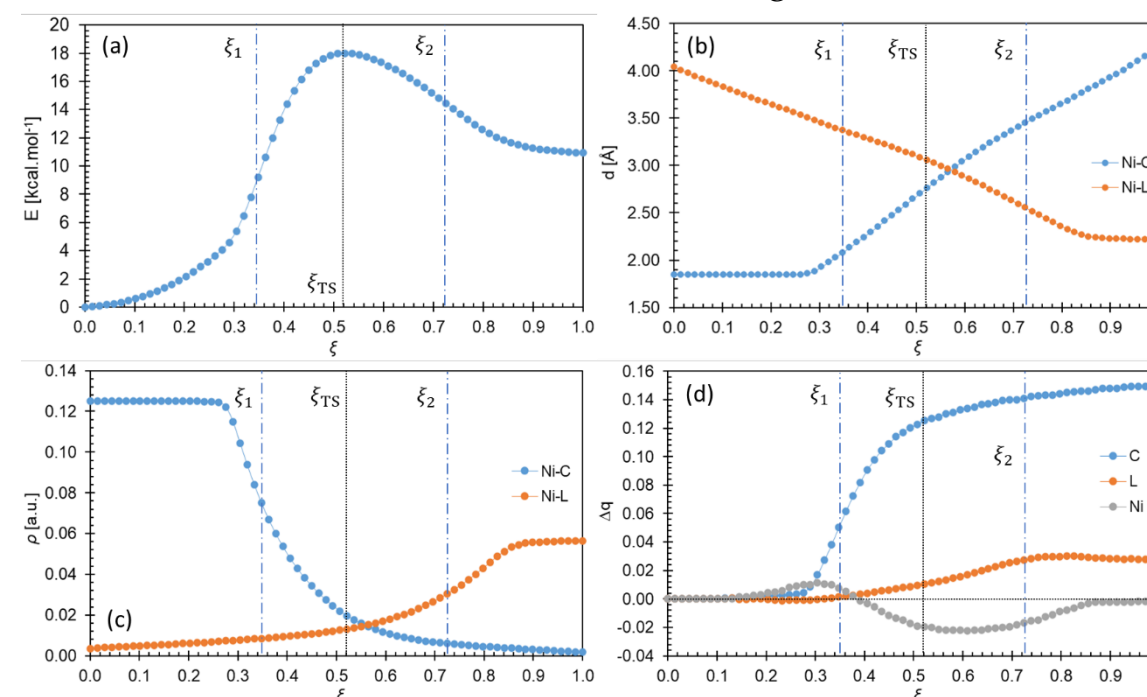
Calculated changes along the reaction path for a carbon monoxide substitution by HCN molecule of (a) reaction energy profile, (b) bond distances change, (c) electron density change at BCP and (d) relative atomic net charge.



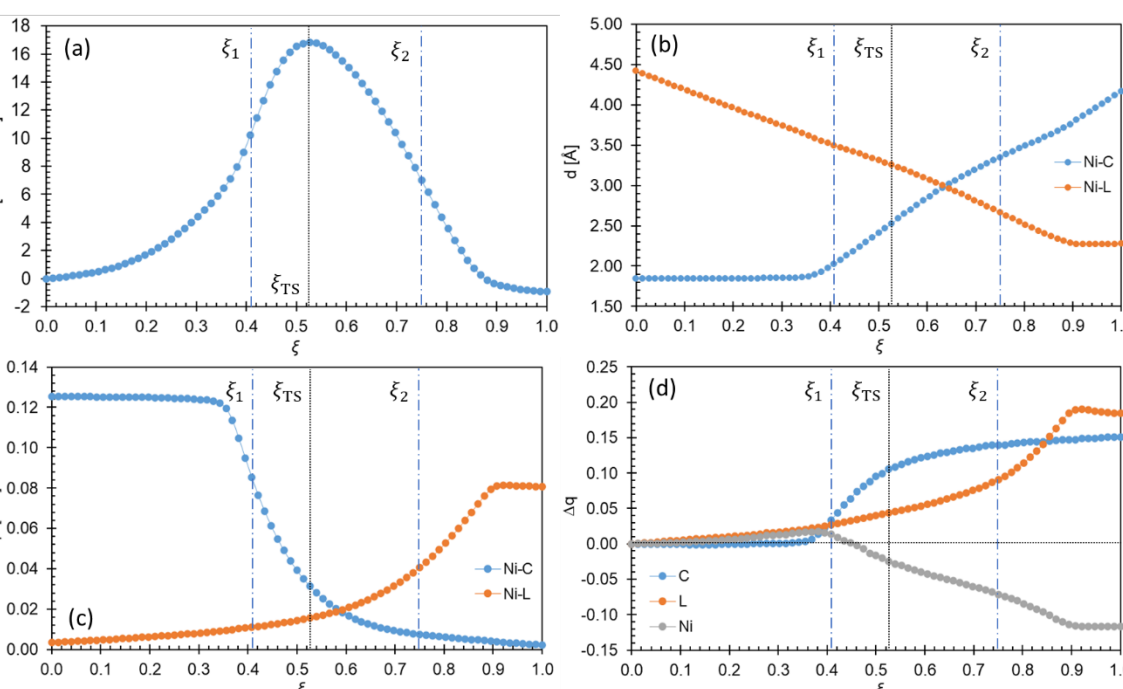
Calculated changes along the reaction path for a carbon monoxide substitution by Py molecule of (a) reaction energy profile, (b) bond distances change, (c) electron density change at BCP and (d) relative atomic net charge.



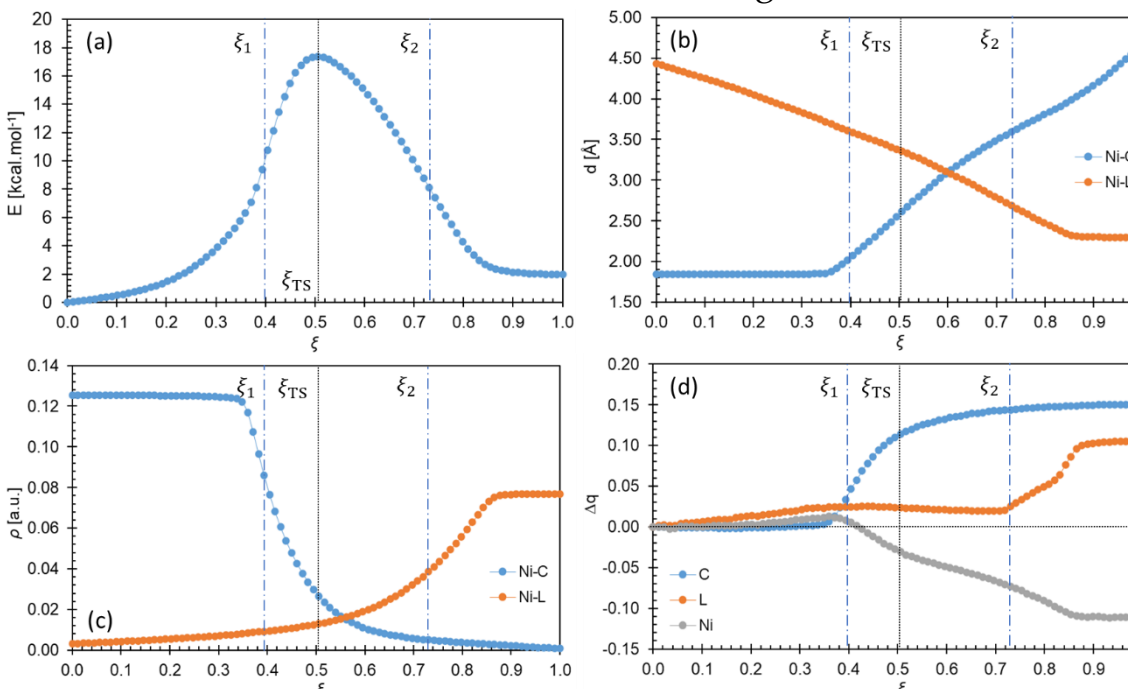
Calculated changes along the reaction path for a carbon monoxide substitution by NMe<sub>3</sub> molecule of (a) reaction energy profile, (b) bond distances change, (c) electron density change at BCP and (d) relative atomic net charge.



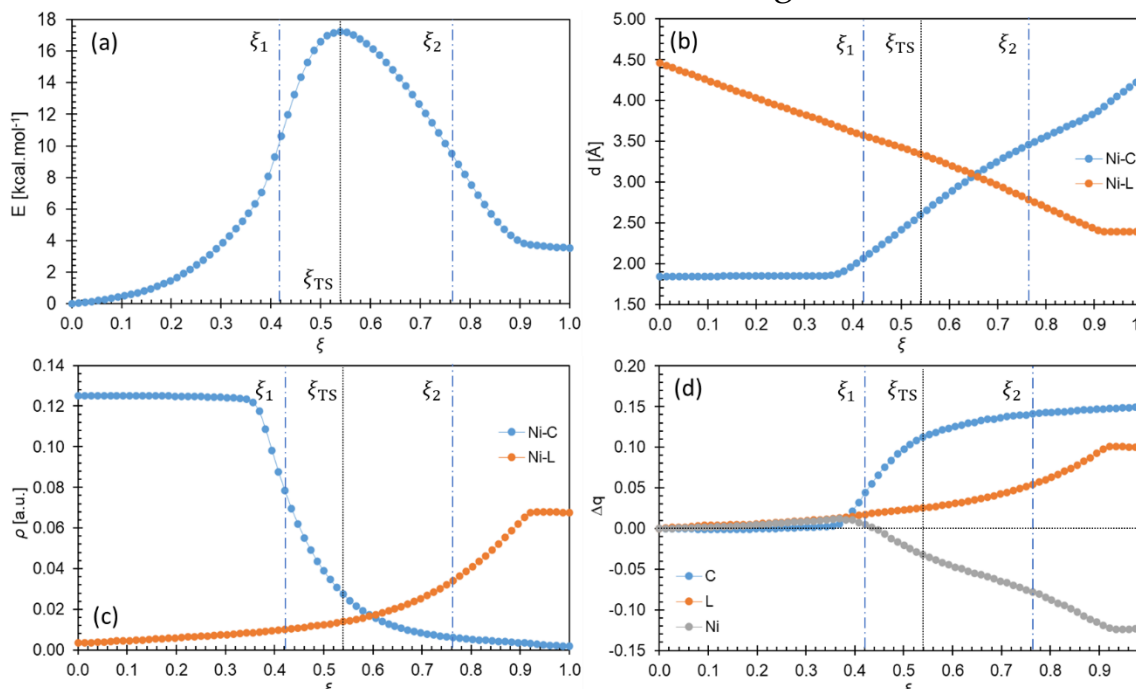
Calculated changes along the reaction path for a carbon monoxide substitution by PMe<sub>3</sub> molecule of (a) reaction energy profile, (b) bond distances change, (c) electron density change at BCP and (d) relative atomic net charge.



Calculated changes along the reaction path for a carbon monoxide substitution by PPh<sub>3</sub> molecule of (a) reaction energy profile, (b) bond distances change, (c) electron density change at BCP and (d) relative atomic net charge.

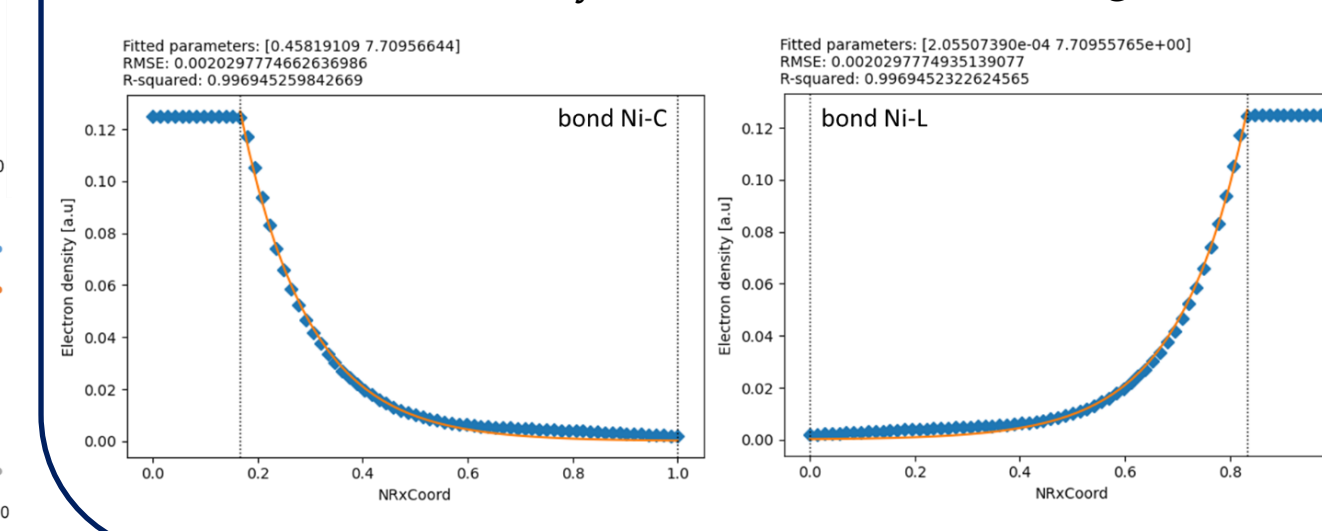


Calculated changes along the reaction path for a carbon monoxide substitution by AsMe<sub>3</sub> molecule of (a) reaction energy profile, (b) bond distances change, (c) electron density change at BCP and (d) relative atomic net charge.

**Fitting example**

Exponential fitting of electron density change at BCP of a breaking Ni-C and a forming Ni-L bond

$$y = a * e^{-b*x} \sim \text{decay} \quad y = a * e^{b*x} \sim \text{growth}$$



Pearson correlation coefficients matrix (green field ( $|r| \geq 0.85$ ) - strong linear relationship, yellow field ( $0.80 \geq |r| \geq 0.85$ ) - medium linear relationship)

	$\Delta E^\ddagger$	$\Delta E^\circ$	$W_1$	$W_2$	$W_3$	$W_4$	$a^a$	$b^b$	$a^c$	$b^d$
$\Delta E^\ddagger$	1.00	0.35	-0.96	0.98	0.18	0.13	-0.75	-0.38	-0.80	0.86
$\Delta E^\circ$	0.35	1.00	-0.20	0.26	0.98	0.96	-0.47	-0.28	0.09	-0.12
$W_1$	-0.96	-0.20	1.00	-0.99	0.00	-0.03	0.64	0.36	0.90	-0.92
$W_2$	0.98	0.26	-0.99	1.00	0.07	0.07	-0.69	-0.37	-0.87	0.91
$W_3$	0.18	0.98	0.00	0.07	1.00	0.95	-0.37	-0.21	0.29	-0.31
$W_4$	0.13	0.96	-0.03	0.07	0.95	1.00	-0.29	-0.21	0.21	-0.29
$a^a$	-0.75	-0.47	0.64	-0.69	-0.37	-0.29	1.00	0.72	0.36	-0.52
$b^b$	-0.38	-0.28	0.36	-0.37	-0.21	-0.21	0.72	1.00	0.22	-0.19
$a^c$	-0.80	0.09	0.90	-0.87	0.29	0.21	0.36	0.22	1.00	-0.93
$b^d$	0.86	-0.12	-0.92	0.91	-0.31	-0.29	-0.52	-0.19	-0.93	1.00

<sup>a</sup> Exponential initial parameter for electron density at BCP of Ni-C bond

<sup>b</sup> Exponential decay rate for electron density at BCP of Ni-C bond

<sup>c</sup> Exponential initial parameter for electron density at BCP of Ni-L bond

<sup>d</sup> Exponential decay rate for electron density at BCP of Ni-L bond

**Key takeaways**

- Energy barrier  $\Delta E^\ddagger$  is mostly influenced by reaction works  $W_1$  and  $W_2$ , and by electron density growth rate of a forming bond. Reaction work  $W_1$  has a negative correlation while reaction work  $W_2$  and electron density growth rate of a forming bond have a positive correlation with the activation energy barrier.
- In order to manipulate the activation energy barrier, for example to lower its value, one must choose an entering ligand which in the reaction of carbon monoxide substitution at Ni(CO)<sub>4</sub> exhibit greater amount of reaction work needed for structural rearrangement  $W_1$  and/or needs a lower amount of  $W_2$  and/or has a slower growth rate of electron density of a forming bond.
- Reaction energies  $\Delta E^\circ$  for this substitution series are predominantly influenced by reaction works  $W_3$  and  $W_4$ . These reaction works have a positive correlation to reaction energies, meaning that with increasing of its values reaction energy also increases.
- Reaction work  $W_1$  has a negative while reaction work  $W_2$  has a positive correlation with electron density growth rate of a forming bond. Thus, meaning that the faster electron density growth needs more energy for of electron rearrangement process ( $W_2$ ) while on the contrary there is less work needed for the structural rearrangement process ( $W_1$ ).